First-principles optical properties of Si/CaF_2 multiple quantum wells

Elena Degoli and Stefano Ossicini
Istituto Nazionale per la Fisica della Materia (INFM) and Dipartimento di Fisica, Università di Modena, Via Campi 213/A, 41100 Modena, Italy

(Received 1 December 1997; revised manuscript received 17 February 1998)

The optical properties of Si/CaF_2 multiple quantum wells are studied *ab initio* by means of the linear-muffin-tin-orbital method. In particular, we investigate the dependence of the optoelectronic properties on the thickness of the Si wells. We find that below a well width of ~20 Å, new transitions appear in the optical region with an evident polarization dependence. The oscillator strength of these transitions shows a dramatic increase as the width of the Si well decreases. A comparison is made with recent experimental work on similar systems. Our results show that quantum confinement and passivation are necessary in order to have photoluminescence in confined silicon-based materials. [S0163-1829(98)04023-5]

I. INTRODUCTION

One of the fastest-growing areas in the field of semiconductor research is that of low-dimensional structures. The properties of these materials show dramatic changes with respect to their bulk counterpart. In particular the observation of bright, visible luminescence in porous Si (PSi) (Ref. 1) has stimulated intense experimental[2] and theoretical[3] work to understand both the energy blueshift and the increased efficiency of luminescence in confined Si structures. In fact, on the basis of extensive experimental evidence, it is the low dimensionality of PSi that is responsible for its peculiar optical properties. However the microscopic structure of PSi is still not well characterized, since the crystallinity, (surface) chemistry, and morphology of PSi are not easy to establish. One way to overcome these difficulties is to fabricate simpler Si-based low-dimensional materials. Several years ago[4–6] we proposed the lattice-matched system $CaF_2/Si/CaF_2$ as the prototype of a well-controlled and ordered Si-based system with a known microscopic structure. Our all-electron calculations for ultrathin Si(111) layers embedded in CaF_2 show that quantum confinement causes a band-gap opening which depends on the Si layer thickness, while Si-Ca hybridization effects at the interface lead to dipole-allowed optical transitions all over the Brillouin zone.[5] In analogy to PSi,[2] the variety of possible low-energy interband transitions might lead to visible radiative recombination. Subsequently, Si/CaF_2 multiple quantum wells (MQW's) which show efficient photoluminescence (PL) at room temperature have been synthesized by molecular-beam epitaxy (MBE).[7,8] The disappearance of the luminescence for Si layers thicker than 25 Å, and the blueshift of the spectra for decreasing thicknesses of the Si layers, are both in agreement with the quantum confinement hypothesis and with the theoretical conclusion of Ref. 5.

Very recently optical-absorption measurements have been performed on these samples[9] and have indicated that the absorption energy of the MQW's (centered around ~2.4 eV) is larger than the luminescence energy (centered around ~ 1.7 eV). This fact, together with experimental observations based on reflection high-energy electron diffraction and extended x-ray-absorption fine structure[6,7] on the structural composition of the MQW's, seems to indicate that these MQW's consist of Si grains with lateral dimensions of about 15–20 Å, rather than of Si ordered layers.[10]

In this paper we present first-principles calculations of the optical properties of the Si/CaF_2 MQW's within the linear-muffin-tin-orbital (LMTO) method in the atomic-sphere approximation (ASA), along the line of the work made on electronic properties presented in Ref. 5. Our aim here is (i) to study the effects of the low dimensionality on the optical properties of Si, (ii) to discuss the experimental findings for the MBE-grown Si/CaF_2 MQW's, and (iii) to investigate, in the light of our results, the possibility of PL in Si-based materials.

The paper is organized as follows: in Sec. II the method for the calculation of the optical properties of the Si/CaF_2 MQW is outlined. Section III is devoted to the presentation and discussion of the optical results, with particular attention to low-dimensionality effects. Conclusions are presented in Sec. IV.

II. ELECTRONIC AND OPTICAL PROPERTIES: THE METHOD

The self-consistent electronic structures of the Si/CaF_2 MQW's are calculated by means of the LMTO-ASA, which has proven to describe correctly the Si/CaF_2 interface properties.[5,11,12] Exchange and correlation effects are included within the density-functional theory in the local-density approximation (LDA). Due to the LDA we underestimate the energy gaps: we obtain 0.56 and 6.96 eV instead of the experimental values of 1.1 and 12.1 eV for bulk Si and CaF_2, respectively. In order to overcome the lack of periodicity perpendicular to the interface, for MQW we use calculations supercells formed by a variable number of Si double layers (DL's), separated by CaF_2 layers (see Fig. 1 of Ref. 5). The number of CaF_2 layers in the calculations has been chosen large enough (at least three layers) to make the central CaF_2 layer exhibits bulklike properties. Throughout, we use the lattice constant of CaF_2 (only 0.6% greater than in bulk Si) except for the interfacial Si-Ca distance, which is taken to be 3.15 Å as found[13,14] experimentally. Our structural model follows the experimental outcomes;[13,14] the first monolayer of CaF_2 loses half of its fluorine atoms leading to the Ca-Si bond at the interface. The interface Ca atoms occupy the T_4 sites; the triangular filled sites on top of the second layer Si atoms, while the F atoms are located on the

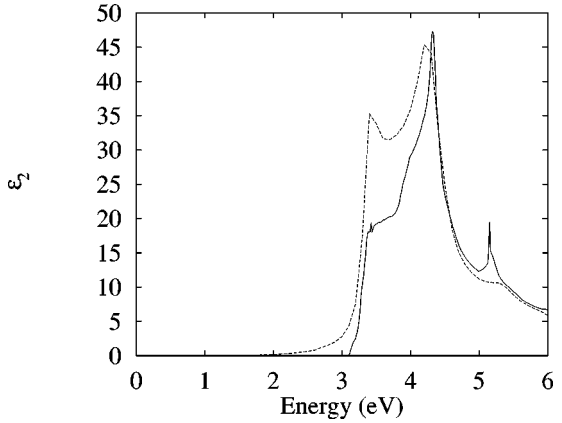

FIG. 1. Imaginary part of the dielectric function ϵ_2 for bulk Si. Solid line: this work; dashed line: experiment (Ref. 17). The theoretical result was blueshifted by 0.5 eV to correct the LDA underestimation of the Si band gap.

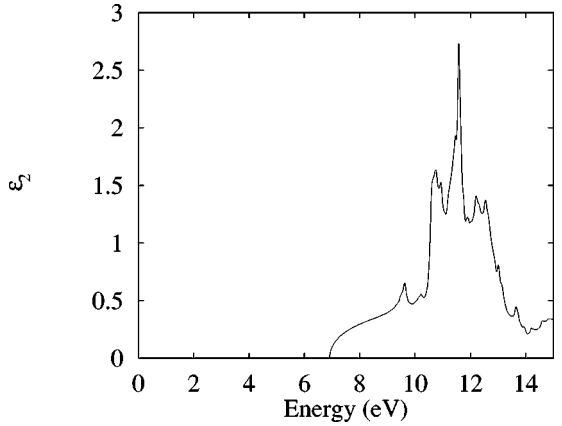

FIG. 2. Calculated imaginary part of the dielectric function ϵ_2 for bulk CaF_2.

H_3 sites, the triangular hollow sites on top of the fourth-layer Si atoms. For further details on the structural model used, the reader is referred to Refs. 4 and 5.

The thickness of the Si wells embedded in CaF_2 ranges from 5.5 to 24.4 Å. The first value corresponds to the case of a single DL of Si embedded in CaF_2, the second to seven DL's of Si. The number of supercell atoms (including empty spheres for close packing) ranges from 15 to 39. Once the self-consistent electronic properties have been calculated, the optical properties of the MQW's have been computed by evaluating the imaginary part of the dielectric function in the optical limit:

$$\epsilon_2^{\alpha}(\omega)=\frac{4\pi^2e^2}{m^2\omega^2}\sum_{v,c}\frac{2}{V}\sum_{k}|\langle\psi_{c,k}|p_{\alpha}|\psi_{v,k}\rangle|^2 \times\delta[E_c(k)-E_v(k)-\hbar\omega], \quad (1)$$

where $\alpha=(x,y,z)$, E_v and E_c denote the energies of the valence $\psi_{v,k}$ and conduction $\psi_{c,k}$ band states at a **k** point, and V is the supercell volume. We have developed a routine for the computation of the optical matrix elements in the gradient representation. The large basis set, that includes angular momentum up to $l=3$, assures the accuracy of the calculation.[15,16] The ϵ_2 is calculated for photon energies up to 20 eV. To perform the summation over **k**, we used the tetrahedron method and a suitable number of **k** points. This number ranges from 128 for the largest supercell to 726 for the smallest one. From the calculated ϵ_2 the real part ϵ_1 is obtained by Kramers-Kronig transformation, after having attached a tail to ϵ_2 for energies greater than 15 eV following Ref. 16.

The optical-absorption coefficient

$$\alpha(\omega)=\frac{\omega}{nc}\epsilon_2(\omega) \quad (2)$$

is directly related to ϵ_2, thus ϵ_2 contains the necessary information about the absorption properties of the material. The knowledge of both ϵ_2 and ϵ_1 allows the determination of the normal-incidence reflectance R and of the real (n) and imaginary (k) parts of the refractive index.

In order to test the reliability of our calculations, we first computed the imaginary and real parts of the dielectric function for bulk Si and bulk CaF_2. The imaginary part of the dielectric function ϵ_2 for bulk Si between 0 and 6 eV is shown in Fig. 1, where it is compared with the experimental result (dashed line) of Aspnes and Studna.[17] To perform this comparison, we shifted our result to the blue by 0.5 eV, in order to overcome the LDA underestimation of the band gap. Our results compare fairly well with the experiment, except for the intensity of the lower-energy peak present in the experimental data. This excitonic peak cannot be correctly described by a one-particle theory and therefore it is also underestimated in other calculations.[18,19]

Regarding the real part of the dielectric function ϵ_1, we found a good agreement with the experimentally derived behavior;[17] in particular, we note that our calculated static dielectric constant $\epsilon_1(0)$ shows a value of 10.53, to be compared with the experimental result of 11.4.[17] For the refraction index we calculate $n=3.25$ with respect to the experimental value of $n=3.8$–4.1.[17]

If we consider bulk CaF_2, our calculated ϵ_2 is shown in Fig. 2 in the 0–15-eV range. We note that our result is in good agreement with previous calculation,[20] and, taking into account the gap underestimation, also with the experimental result.[21] We also obtain, even for bulk CaF_2, a calculated static dielectric constant $\epsilon_1(0)$ value of 1.51, in good agreement with the reported experimental result of 1.5.[21] These results allows us to discuss the optical properties of the Si/CaF_2 MQW's looking in particular at their dependence on the thickness of the Si wells. The comparison between bulk and slab results gives the possibility to enucleate features entirely due to the confinement effect.

III. MQW'S OPTICAL PROPERTIES

A. Imaginary part of the dielectric function ϵ_2

In this section we will discuss the effect of layering on the optical properties of quantum Si slabs. However, before presenting our results on the optical properties, it is worthwhile to summarize the major outcomes of the calculation of the electronic properties of the Si/CaF_2 MQW's.[4–7] The major changes in the electronic properties of the MQW's with respect to bulk Si results occur in the energy region around the

TABLE I. Calculated energy gaps and lowest direct transitions at Γ for the different considered MQW's. The values are compared with that of bulk Si.

Lattice	Size (Å)	Gap (eV)	ΔE_{cv} (eV)
Si bulk		0.56	2.59
Seven DL's	24.4	0.56	1.14
Four DL's	14.9	0.63	1.31
Two DL's	8.7	1.24	1.81
One DL	5.5	0.76	2.13

gap, while, deeper in the valence band, one can recognize the almost unaffected Si and CaF_2 band structures. There are three main effects related to the layering to be noticed: (i) the band gap increases, i.e., there is a blueshift of the bulk energy gap due to the confinement; (ii) the lowest conduction-band width is largely reduced, i.e., the k dispersion for this band is quite low; and (iii) the edge of the valence band is shifted from Γ to finite in-plane wave vectors (i.e., in the k space the locations of the valence-band maximum and of the conduction-band minimum are now nearer with respect to the Si bulk situation), but the gap remains still indirect. Table I collects our results for the energy gap and for the energy of the lowest direct transition at Γ for the different considered superlattices. Even for the thicker slab, the bulklike situation is not recovered: in fact an interface state appears just below the conduction band at Γ, together with an interface state in the valence-band region that becomes the highest valence state in the thinner slabs (one DL and two DL's). These two interface states are the bonding-antibonding states resulting from the Ca-Si bond at the interface. The bonding state is particularly easy to identify in the case of one DL, where it appears clearly above the double-degenerate valence-band edge of Si at Γ, thus reducing the energy gap. It should be noted that the Si-Ca bond at the interface is somewhat intermediate between the covalent Si-Si bond and the ionic Ca-F bond. Therefore, the bonding-antibonding states are not completely removed from the gap, as in the case of H-saturated Si structure. The H-Si bond, being highly covalent, instead gives rise to a much larger bonding-antibonding energy separation, and pushes the interface states inside the Si valence and conduction bands.[6,22,23]

In Fig. 3, we show the dependence of our calculated imaginary part of the dielectric function ϵ_2 on the thickness of the Si slab embedded in CaF_2. For comparison, we also report in Fig. 3 our ϵ_2 result for bulk Si (solid line). For ease of discussion, three main regions have been identified, according to the different portions of ϵ_2, and have been indicated with labels from I to III. Region III between $\sim$10 and $\sim$14 eV is mainly related to the CaF_2 contribution to the ϵ_2 of the MQW's (see also Fig. 2 in this energy region). We note that the features in this region gain weight with respect to region II (between $\sim$3 and $\sim$6 eV) on reducing the thickness of the Si slab; clearly this is due to the increase in weight of the CaF_2 side with respect to Si in the MQW's. In fact, region II is directly related to the crystalline Si contribution to the ϵ_2 of the MQW's; this is the region to be compared directly to the Si bulk result. The main characteristic of region II is the reduction of the maximum value for ϵ_2. This reduction follows exactly the lowering in thickness

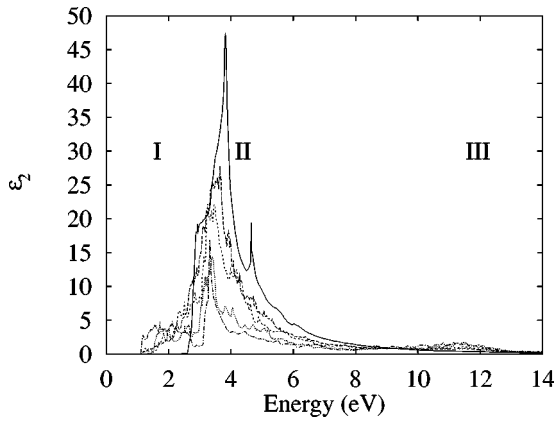

FIG. 3. Calculated imaginary part of the dielectric function ϵ_2 for Si/CaF_2 MQW's. Large dashed line: seven Si DL's; small dashed line: four Si DL's; dotted line: two Si DL's; dash-dotted line: one Si DL. The values are compared with that of bulk Si: solid line.

of the Si slab, and it is due to the confinement effect. Similar results have been obtained theoretically for hydrogen-saturated Si quantum wells,[23] wires,[24,25] and dots,[19] and experimentally in the case of PSi,[26] where it is widely accepted that the structure is mainly constituted of Si quantum wires and dots. In particular we note that the E_1 spectral feature at $\sim$3 eV in bulk Si is weakened and shifts to the blue as a consequence of quantum confinement effect, whereas the E_2 peak shows a redshift. A different behavior with respect to the influence of quantum confinement of the critical points of the band structure of Si has been demonstrated in the case of extremely thin layers of PSi.[27]

More important for our discussion is the low-energy region I (between $\sim$1 eV and $\sim$2.5 eV). Here features appear which are completely absent in the case of bulk Si. If we take into account the $\sim$0.5-eV LDA underestimation of the Si energy gap, this is the optical region of interest. First of all, we remember that experiments on Si/CaF_2 MQW's (Refs. 7–9) show PL and absorption gaps even in an energy region between $\sim$1.5 and $\sim$2.5 eV,[7–9] in agreement with our results. Moreover, in Fig. 4 we show a blowup of the low-energy part of ϵ_2 in the 1–2-eV range. A blueshift, consistent with quantum confinement, of the onset of ϵ_2 for decreasing Si thickness is clearly evident. The only exception is the system with one DL of Si, for which the bonding Si-Ca interface state emerges from the valence band, thus reducing the band gap, as shown in Refs. 5 and 6 (see also Table I) and discussed above. Second, the features of ϵ_2 in this region are very smooth for the larger Si slab (seven DL's), while their weight increases with confinement.

Another important aspect of the imaginary parts of the MQW's dielectric functions is related to their anisotropic behavior. Figure 5 shows the contribution to ϵ_2 for different polarization direction parallel (solid lines) and perpendicular (dashed lines) to the plane of the quantum well for the Si seven-DL and Si two-DL cases. We see that in the larger quantum well the two components are quite similar, as expected for a situation that resembles that of bulk Si. Instead for the two-DL case, the main peak is mostly due to the parallel contribution, whereas the perpendicular component (the direction of confinement) shows important weight in the

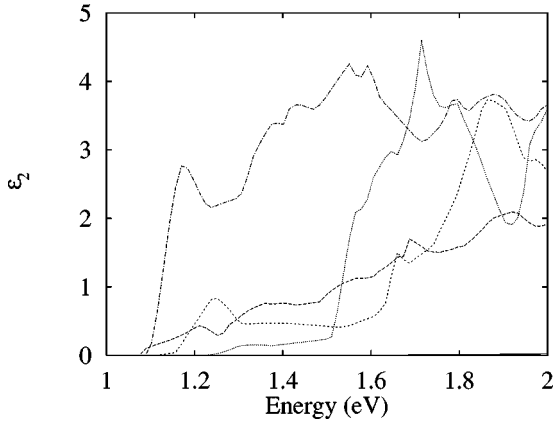

FIG. 4. Same as in Fig. 3, in the 1–2 energy range.

low-energy (optical) region. The confinement induces an optical response that clearly depends on the polarization direction, this fact could be confirmed by experimental observations.

In order to enucleate the transitions which play an important role in the low-energy region, in Fig. 6 we show (for the two-DL Si case) the total ϵ_2 (solid line) together with the contributions due to the transitions from the last valence band to the first conduction band (short dashed line) and from the last two valence bands to the first two conduction bands (long dashed line). From the figure, the predominant role played by the band edges is evident, in particular for the interface states in the optical region; we remember that for very thin Si slabs the last occupied and first unoccupied states are mostly related to the interface states.

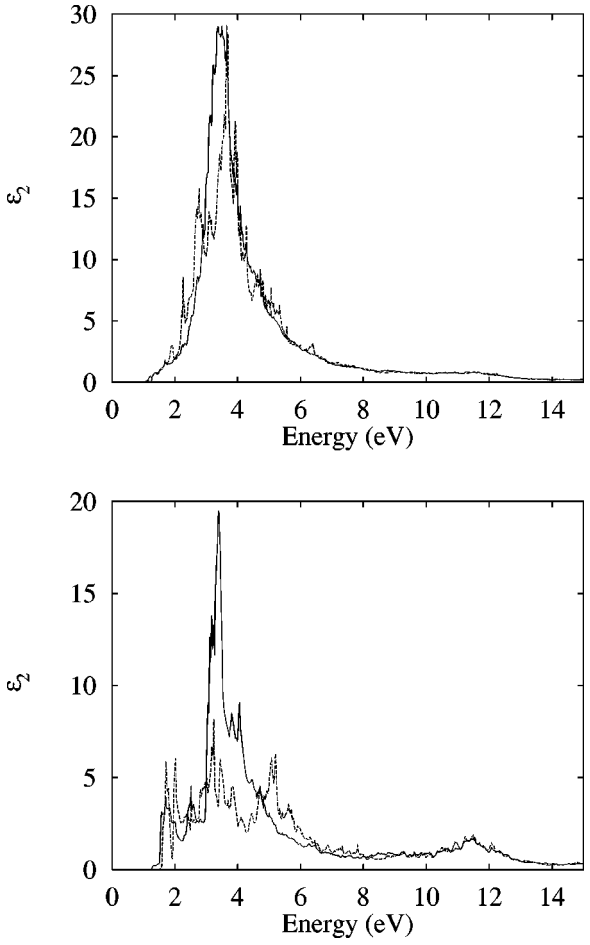

FIG. 5. Calculated imaginary part of the dielectric function ϵ_2 for Si/CaF_2 MQW's. Polarization parallel to the Si layers: solid line; polarization perpendicular to the Si layers: dashed line. Top panel: seven Si DL's; bottom panel: two Si DL's.

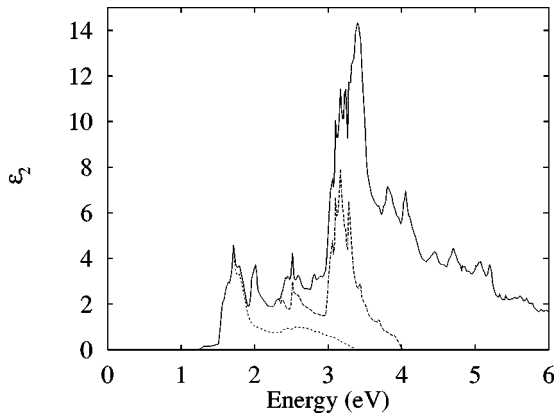

FIG. 6. The most important interband contributions to the imaginary part of the dielectric function ϵ_2 of the 2-DL Si/CaF_2 MQW's. Solid line: total ϵ_2; short dashed line: contribution from the transition between the last occupied state and the first unoccupied one; long dashed line: the same considering the last two occupied states and the first two empty states.

The origin of the peaks, which are responsible of the anisotropic behavior of the optical properties, is related to the presence of significant matrix elements between particular states which are located at, or just below, the top of the valence band and at, or just above, the bottom of the conduction band. The top valence states are mainly *p* Si-derived states, whereas the bottom conduction ones are mainly *p* Si- and *s* and *d* Ca-derived states. The calculated oscillator strengths for the transitions between these states are listed and compared in Table II. It is worthwhile to note that the oscillator strengths for the matrix elements between these states increase very rapidly as the thickness of the slabs decreases, and that, for layers with thickness less than 20 Å, they are of the same order of magnitude as the direct transition at Γ in bulk Si and only one order of magnitude smaller than those for GaAs. It is tempting to link directly these transitions to the PL peaks observed in Si/CaF_2 MQW's.[7,8] The reason for the rapid increase of the dipole strength with decreasing slab thickness is due to the different localization of the states involved in the transition. The intensity of the oscillator strength for a transition between two states de-

TABLE II. Calculated energies and oscillator strengths for significant direct transitions at Γ for the different considered MQW's. The values are compared with that of bulk Si.

Lattice	Size (Å)	ΔE_{cv} (eV)	f_{cv}
Si bulk		2.59	2.53
Seven DL's	24.4	1.44	0.004
Four DL's	14.9	1.73	0.42
Two DL's	8.7	1.81	0.66
One DL	5.5	2.13	0.72

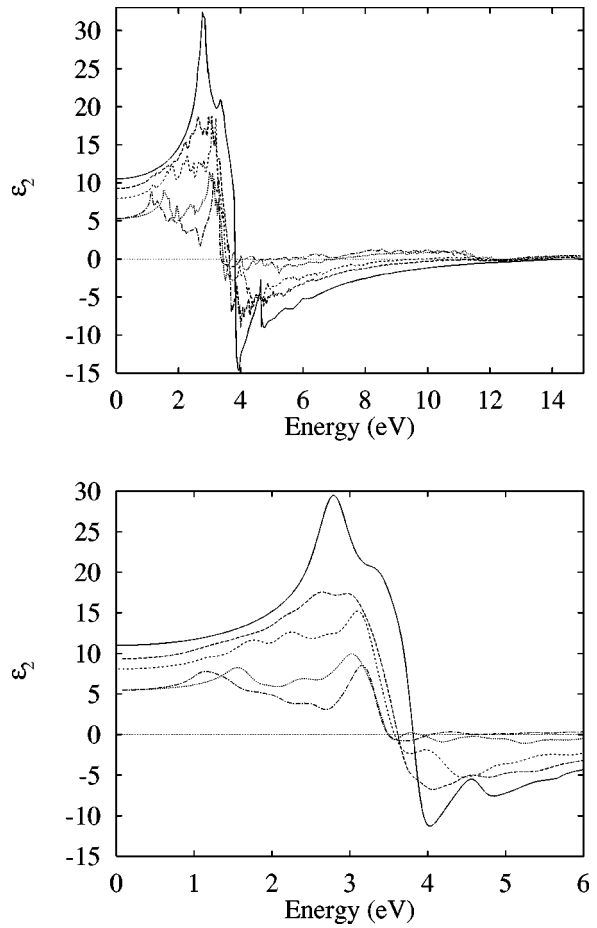

FIG. 7. Real part of the dielectric function ϵ_1 for Si/CaF_2 MQW's. Large dashed line: seven Si DL's; small dashed line: four Si DL's; dotted line: two Si DL's; dash-dotted line: one Si DL. The values are compared with that of bulk Si: solid line. Top panel: theoretical results; bottom panel: the same dressed by a Gaussian broadening of 0.1 eV.

pends not only on the localization in the reciprocal k space but also on the localization in the real space, i.e., in which layers these states are localized. For very thin slabs these states are both strongly localized at the interface, whereas for the seven-DL slab case they are spread out over the entire Si slab. Thus the optical transition matrix element which indicates the probability of the transition decrease as the number of Si layers is made larger.

B. Real part of the dielectric function ϵ_1

The calculated values of the real part of the dielectric function ϵ_1 for the Si/CaF_2 MQW's are shown in Fig. 7, together with the corresponding results for bulk Si. They are obtained by use of Kramers-Kronig transformation, as stated in Sec. II. In order to have a better insight into the behavior of ϵ_1, the bottom panel of Fig. 7 shows our results dressed with a Gaussian broadening of 0.1 eV.

A strong reduction of the maximum value of ϵ_1 in going from bulk Si to quantum wells is clear; moreover, we observe that the high-energy shoulder becomes more important with respect to the main peak in the MQW case. The static dielectric constants of the Si quantum slabs $\epsilon_1(0)$ are considerably smaller than that of bulk Si, reflecting quantum confinement effects. The values are reported in Table III. The decrease in the static dielectric constant of Si quantum slabs is consistent with the results of the theoretical analysis reported by Tsu and co-workers[28,29] and Wang and Zunger[19] for Si quantum dots, and by Ossicini *et al.*[30] for Si quantum wires. From the experimental point of view, a similar large reduction of $\epsilon_1(0)$ (from 11.4 to $\sim$2.5) has been observed in PSi.[26] The importance of the reduction of the dielectric constant in order to use Si for optoelectronic purposes was pointed out and discussed in Refs. 28 and 29. Another interesting implication of this reduction is that the exciton recombination energy in the ultrathin Si slabs could be significantly increased. In the case of Si quantum dots, Wang and Zunger found that for quantum dots whose radius is less than 20 Å the electron-hole pair is confined by the physical dimension of the dot, not by the Coulomb attraction.[19]

TABLE III. Real part of the dielectric function, and real part of the refraction index and reflectivity calculated at $\omega=0$ for the different considered MQW's. The values are compared with that of bulk Si.

Lattice	$\epsilon_1(0)$	$n(0)$	$R(0)$
Si bulk	10.53	3.24	0.28
Seven DL's	9.26	3.04	0.26
Four DL's	7.98	2.82	0.23
Two DL's	5.32	2.31	0.16
One DL	5.32	2.31	0.16

C. Other optical parameters

Figures 8, 9, and 10 report our calculated results for the refraction index

$$n(\omega)=(\tfrac{1}{2}\{[\epsilon_1^2(\omega)+\epsilon_2^2(\omega)]^{1/2}+\epsilon_1(\omega)\})^{1/2}, \qquad (3)$$

the extinction coefficient

$$K(\omega)=(\tfrac{1}{2}\{[\epsilon_1^2(\omega)+\epsilon_2^2(\omega)]^{1/2}-\epsilon_1(\omega)\})^{1/2}, \qquad (4)$$

and the reflectivity

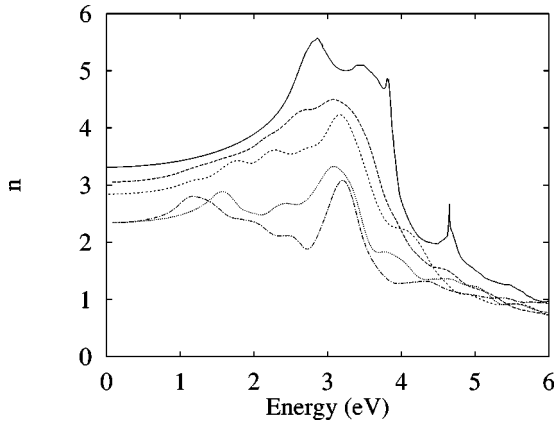

FIG. 8. Real part of refractive index n for Si/CaF_2 MQW's. Large dashed line: seven Si DL's; small dashed line: four Si DL's; dotted line: two Si DL's; dash-dotted line: one Si DL. The values are compared with that of bulk Si: solid line.

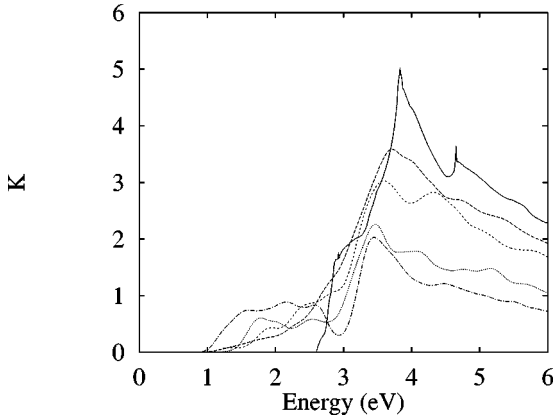

FIG. 9. Imaginary part of refractive index K for Si/CaF_2 MQW's. Large dashed line: seven Si DL's; small dashed line: four Si DL's; dotted line: two Si DL's; dash-dotted line: one Si DL. The values are compared with that of bulk Si: solid line.

$$R(\omega)=\frac{[n(\omega)-1]^2+K^2(\omega)}{[n(\omega)+1]^2+K^2}. \tag{5}$$

The values of $n(0)$ and $R(0)$ are reported in Table III. It should be observed that often it is the reflectivity that is the measured quantity in the optical characterizations.

The dependence of the reflectivity, the extinction coefficient, and the refraction index on the Si layer thickness is quite evident. Once more our calculated behavior for these parameters is similar, regarding the dimensionality effects, to that reported in Refs. 26 and 31 for porous silicon. A strong reduction in the intensity for both reflectivity and refraction index is clearly present. In particular low refraction index values can be seen to be predicted for the ultrathin Si layer. The dependence of the refraction index values on the dimension of the Si slab could be in principle used for optoelectronic applications in multilayer structures, where one alternates, in a CaF_2 matrix, Si slab of different thicknesses (see for example the case of porous Si multilayers[32]). The extinction coefficient shows features not present in the Si bulk case, in the low-energy optical region.

The calculated absorption spectra for our Si/CaF_2 MQW's [see Eq. (2)] are reported in Fig. 11 together with the corresponding results for bulk Si. Similarly to the experimental results of Bassani *et al.*[9] performed on fresh multilayers (to avoid the effect of aging in air, which leads to an oxidation of the Si layers), we observe a blueshift of the onset, and moreover a decrease of the optical absorption with decreasing Si layer thickness. The only discrepancy between theory and experiment is thus related to the difference in energy between absorption and luminescence. We do not take into account any complicated effects that can play a role in the luminescence processes, thus our results for the optical properties reflect directly the electronic properties in the ground state. In their experiment, Bassani *et al.*[9] assumed for the determination of the optical pseudogap the usual Tauc linear relationship for a semiconductor with an indirect band gap, and obtained values for the optical gaps, which increases as the Si layer thickness decrease but that are ~ 1 eV above the PL peaks. This fact led to their conclusion that the MQW's contain Si grains of nanodimensions rather than two-dimensional Si layers.

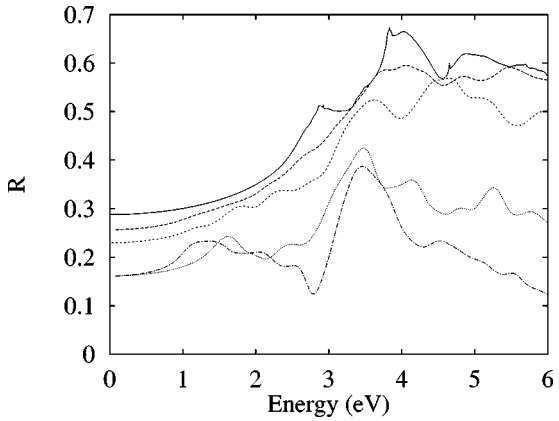

FIG. 10. Reflectivity R for Si/CaF_2 MQW's. Large dashed line: seven Si DL's; small dashed line: four Si DL's; dotted line: two Si DL's; dash-dotted line: one Si DL. The values are compared with that of bulk Si: solid line.

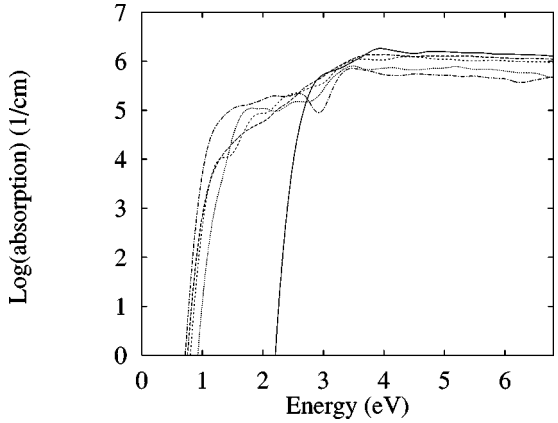

FIG. 11. Log of the absorption coefficient (cm^{-1}). Large dashed line: seven Si DL's; small dashed line: four Si DL's; dotted line: two Si DL's; dash-dotted line: one Si DL. The values are compared with that of bulk Si: solid line.

Very recently we have studied the optical properties of hydrogen-saturated Si clusters showing that clusters of ~ 20-Å size in the ground state have gaps of the order of 2.5 eV, whereas in the excited state they relax to locally distorted equilibrium configurations, giving rise to transitions involving localized states that lower (~ 1 eV) the emission threshold.[33] An investigation of the possible link between this calculation and the experimental results of Bassani *et al.* is in progress.

IV. SUMMARY AND CONCLUSIONS

In this paper we have presented the results of first-principles calculations of the optical properties of Si/CaF_2 MQW's. In particular, we have studied how the optical properties of Si slabs (embedded in a CaF_2 matrix) change, depending on their thickness. We have first computed the imaginary part of the dielectric function ϵ_2 and then, using Kramers-Kronig analysis, the real part of the dielectric function ϵ_1 and the other optical parameters: the refraction index, the extinction coefficient, the reflectivity, and the absorption. Through a careful comparison with the corresponding results for bulk Si and bulk CaF_2 it was possible to enucleate the

role of quantum confinement in determining the optical and electronic properties of these superlattices. We have shown that the optoelectronic spectrum of the Si layers is affected both by confinement, yielding a blueshift of the energy gap, and by hybridization effects with the passivating Ca atoms, leading to the presence of a high joint density of states all over the Brillouin zone. The major outcome of this work is that for Si slab dimensions less than ~ 20 Å, interesting transitions appear in the optical region, with oscillator strengths which show a dramatic increase as the slabs width decreases. Moreover, the static dielectric constants for the ultrathin slabs are considerably smaller than that for bulk Si; this fact can be important for optoelectronic applications. These results are also clearly evident in the behavior of the other optical parameters.

Our results provide a possible explanation of the luminescence properties displayed by the Si/CaF_2 superlattices produced by MBE by D'Avitaya and co-workers;[7–9] even though the experimental difference between absorption and luminescence remains to be explained. Nevertheless our *ab initio* result on the dependence of the optical properties of Si on layer thickness has important general consequences from an experimental point of view. Provided that Si layers are well passivated (dangling bonds saturated by H,O, SiO_2, CaF_2, etc.) and well confined (dimension of the order of 10–25 Å), they originate transitions in the optical region. The recent observation of PL from Si/SiO_2 superlattices[34] supports this conclusion.

ACKNOWLEDGMENTS

This work was supported by Consiglio Nazionale delle Ricerche (CNR), Italy, and has benefited from collaborations within the Network on ''Ab-initio (from electronic structure) calculation of complex processes in materials'' (Contract No. ERBCHRXCT930369). We are grateful to A. Fasolino, C. Arcangeli, L. Vervoort, F. Bassani, and F. Arnaud D'Avitaya for useful discussions.

[1] L. T. Canham, Appl. Phys. Lett. **57**, 1046 (1990).
[2] For a recent review, see Y. Kanemitsu, Phys. Rep. **263**, 1 (1995).
[3] For a recent review, see G. J. John and V. A. Singh, Phys. Rep. **263**, 93 (1995).
[4] S. Ossicini, A. Fasolino, and F. Bernardini, in *Optical Properties of Low Dimensional Silicon Structures*, edited by D. Bensahel, L. T. Canham, and S. Ossicini (Kluwer, Dordrecht, 1993), p. 219.
[5] S. Ossicini, A. Fasolino, and F. Bernardini, Phys. Rev. Lett. **72**, 1044 (1994).
[6] S. Ossicini, A. Fasolino, and F. Bernardini, Phys. Status Solidi B **190**, 117 (1995)
[7] F. Arnaud D'Avitaya, L. Vervoort, S. Ossicini, A. Fasolino, and F. Bernardini, Europhys. Lett. **31**, 25 (1995).
[8] L. Vervoort, F. Bassani, I. Mihalcescu, J. C. Vial, and F. A. D'Avitaya, Phys. Status Solidi B **190**, 123 (1995).
[9] F. Bassani, L. Vervoort, I. Mihalcescu, J. C. Vial, and F. Arnaud D'Avitaya, J. Appl. Phys. **79**, 4066 (1996); F. Bassani, I. Mihalcescu, J. C. Vial, and F. Arnaud D'Avitaya, Appl. Surf. Sci. **117/118**, 670 (1997).
[10] A. B. Filonov, A. N. Kholod, V. A. Novikov, V. E. Borisenko, L. Vervoort, F. Bassani, A. Saul, and F. Arnaud D'Avitaya, Appl. Phys. Lett. **70**, 744 (1997).
[11] S. Ossicini, C. Arcangeli, and O. Bisi, Phys. Rev. B **43**, 9823 (1991).
[12] S. Ossicini, C. Arcangeli, and O. Bisi, Surf. Sci. **251/252**, 462 (1991).
[13] R. M. Tromp and M. C. Reuter, Phys. Rev. Lett. **61**, 1756 (1988).
[14] J. Zegenhagen and J. R. Patel, Phys. Rev. B **41**, 5315 (1990).
[15] Yu. A. Uspenski, E. G. Maksimov, S. N. Rashkeev, and I. I. Mazin, Z. Phys. B **53**, 263 (1983).
[16] M. Alouani, L. Brey, and N. E. Christensen, Phys. Rev. B **37**, 1167 (1988).
[17] D. E. Aspnes and A. A. Studna, Phys. Rev. B **27**, 985 (1983).
[18] C. Tserbak, H. M. Polatoglou, and G. Theodorou, Phys. Rev. B **47**, 7104 (1993).
[19] L. Wang Wang and A. Zunger, Phys. Rev. Lett. **73**, 1039 (1994).
[20] Fanqi Gan, Yong-Nian Xu, Ming-Zhu Huang, W. Y. Ching, and J. G. Harrison, Phys. Rev. B **45**, 8248 (1992).
[21] J. Barth, R. L. Johnson, and M. Cardona, Phys. Rev. B **41**, 3291 (1990).
[22] C. G. Van de Walle and J. Northrup, Phys. Rev. Lett. **70**, 1116 (1993).
[23] Sun-Ghil Lee, Byoung-Ho Cheong, Keun-Ho Lee, and K. J. Chang, Phys. Rev. B **51**, 1762 (1995).
[24] L. Dorigoni, O. Bisi, F. Bernardini, and S. Ossicini, Phys. Rev. B **53**, 4557 (1996).
[25] S. Ossicini, C. M. Bertoni, M. Biagini, A. Lugli, G. Roma, and O. Bisi, Thin Solid Films **297**, 154 (1997).
[26] N. Koshida, H. Koyama, Y. Suda, Y. Yamamoto, M. Araki, T. Saito, K. Sato, N. Sata, and S. Shin, Appl. Phys. Lett. **63**, 2774 (1993).
[27] M. Ben-Chorin, B. Averboukh, D. Kovalev, G. Polisski, and F. Koch, Phys. Rev. Lett. **77**, 763 (1996).
[28] R. Tsu, L. Ioriatti, J. F. Harvey, H. Shen, and R. A. Lux, in *Microcrystalline Semiconductors: Materials Science & Devices*, edited by P. M. Fauchet, C. C. Tsai, L. T. Canham, I. Shimizu, and Y. Aoyagi, MRS Symposia Proceedings No. 283 (Materials Research Society, Pittsburgh, 1993), p. 437.
[29] R. Tsu and D. Babic, in *Optical Properties of Low Dimensional Silicon Structures* (Ref. 4), p. 203.
[30] S. Ossicini, M. Biagini, C. M. Bertoni, G. Roma, and O. Bisi, in *Advances in Microcrystalline and Nanocrystalline Semiconductors*, edited by R. W. Collins, P. M. Fauchet, I. Shimizu, J. C. Vial, T. Shimaola, and A. P. Alivigatos, MRS Symposia Proceedings No. 452 (Materials Research Society, Pittsburgh, 1997), p. 63.
[31] C. Pickering, in *Porous Silicon*, edited by Zhe Chuan Feng and R. Tsu (World Scientific, New York, 1995), p. 3.
[32] L. Pavesi, R. Guardini, and C. Mazzoleni, Solid State Commun. **97**, 1051 (1996).
[33] R. Baierle, M. J. Caldas, E. Molinari, and S. Ossicini, Solid State Commun. **102**, 545 (1997).
[34] Z. H. Lu, D. J. Lockwood, and J.-M. Baribeau, Nature (London) **378**, 258 (1995).